

SUPPLEMENTAL DATA

Humanization of anti-TAG72 huCC49 antibody. The humanized variable domains of the anti-TAG72 huCC49 delta CH2 mAb was obtained from the literature (1). The amino acid sequence (1 letter code) of the immunoglobulin variable domains are listed:

Variable light domain:

DIVMSQSPDSLAVSLGERVTLNCKSSQSLLYSGNQKNYLAWYQQKPGQSPKLLIYWAS
ARESGVPDRFSGSGSGTDFTLTISVQAEDVAVYYCQQYYSYPLTFGAGTKLELKRTV
AAPSVFIFPPSDEQLKSGTASVVCLLNNFYPREAKVQWKVDNALQSGNSQESVTEQDS
KDSTYLSSTLTLSKADYEKHKVYACEVTHQGLSSPVTKSFNRGEC

Variable heavy domain:

QVQLVQSGAEVVKPGASVKISCKASGYTFTDHAHVVKQNPGRLEWIGYFSP
GNDDFKYNERFKGKATLTADTSASTAYVELSSLRSEDVAVYFCTRSLNMAYWGQGLTV
TVSSASTKGPSVFPLAPSSKSTSGGTAALGCLVKDYFPEPVTVSWNSGALTSGVHTFP
AVLQSSGLYSLSSVTVPSSSLGTQTYICNVNHKPSNTKVDKKV

The genes encoding the huCC49 delta CH2 were reformatted into a full length human IgG1 mAb by cDNA synthesis (GeneArt Gene Synthesis, ThermoFisher). The light and heavy chains were cloned into the dual chain pEE12/6 expression vector (Lonza, Basel, Switzerland). The huCC49 was transiently expressed in EXPI293 cells (Life Technologies) and the 6 day cell culture supernatant was purified by Protein A (Sigma Millipore, Burlington, MA) and ceramic hydroxyapatite (Bio-Rad, Hercules, CA) chromatography. The purified antibody was characterized by SDS-PAGE and size exclusion chromatography using Superdex 200 (GE Healthcare Life Sciences, Pittsburgh, PA) and showed a purity greater than 98%. Kinetic affinity analysis was conducted by surface plasmon resonance on a Biacore X100 (GE Healthcare). Recombinant TAG-72 antigen (Bio-Rad) was immobilized on a CM-5 chip, and serial concentrations of muCC49 mAb or huCC49 mAb flowed over the chip. The K_D for the muCC49 mAb was 2.5×10^{-8} and huCC49 mAb was 2.3×10^{-8} .

References

1. Braslawski, G.R. et al., US Patent No. 7,319,139, Jan 15, 2008.

Absorbed Dose calculations.

Absorbed Dose calculations.

The alpha-particle energy of a single nucleus ^{225}Ac in 1 disintegration was calculated as 27.65 MeV, which accounts for over 90% of the energy released [28]. Using the high LET 27.65 MeV energy per disintegration, the joules released in 1 day from 1 kBq of ^{225}Ac is 3.8×10^{-4} J. With a half-life of 10 days, the decay-corrected energy released over 38 days is $E_{kBq} = 5.12 \times 10^{-3}$ J per kBq. The average weight measured from a biodistribution study done in parallel with the therapy studies was used to calculate absorbed dose in Gray (Gy). For the single dose study, the biodistribution group was given 1 dose of 3.7 kBq and 2 mice from this group were euthanized per time point, and the tumor weight was measured. For the multi-dose study, the biodistribution group was given multiple doses of either ^{225}Ac -huCC49 or ^{225}Ac -untargeted control antibody and 2 mice from each group were euthanized per time point, at which point the tumor weights were measured. Because not all of the injected dose reaches the tumor, to calculate the amount of energy (E') released in the tumor, the percent of injected dose measured in the tumor is used to adjust the dose-specific energy:

$$E' = \sum_{i=1}^N \int_{t_i}^{t_f} \alpha_i E_{kBq} e^{-\left(\frac{\ln 2}{t_{1/2}}\right)t} dt$$

where the injected dose measured in the tumor after dose i (α_i), is given by the biodistribution studies done for both huCC49 and the untargeted control antibody. The injected dose in the tumor after each dose in the multi-therapy treatment was determined by the ^{111}In biodistribution study (**Figure 4C**). The total injected dose is the sum of the individual doses $D = \sum_{i=1}^N D^i$ (Single dose: 1.85 kBq, 3.7 kBq, or 7.4 kBq; Multi-treatment: 1.85 kBq (x1) + 0.70 kBq (x5)). The percent of the injected dose in the tumor after a single dose of ^{225}Ac -huCC49 was $D^1=5.15\%$. For dose 5, in the multi-treatment therapy, the injected dose was extrapolated based on slope of the line of the surrounding data points ($\alpha_i=.394t-2.86$ $\alpha_5 = 0.0935$), as no biodistribution was done for that time point.

Calculation of tumor growth rate and survival for 5.4 kBq single dose.

Note: This calculation was added in response to review.

Because several factors contribute to overall survival, including tumor burden, treatment toxicity, and inter-individual biological variability, we consider an analysis of tumor growth rates, which is much more consistent across mice and treatment conditions.

We begin by transforming the tumor volume data into the radius of a sphere with an equivalent volume with the formula:

$$r = \left(\frac{3V}{4\pi}\right)^{1/3}$$

For all calculations, we use the average tumor volume across all mice for each time point and treatment condition.

Multiple groups and mathematical models have shown that the radius of untreated tumor growth can grow linearly over time. We can see this in our data for the untreated control arms in both the single and multi-dose experiments. Linear regression of the tumor radius over time has a correlation coefficient of $r > 0.99$. The multi-dose controls have been scaled to have the same initial tumor radius as the single dose controls (**Supplemental Figure S8**).

Now that we have established that in our model, tumor radius grows linearly over time if untreated, we introduce the concept of a fatal (or maximal) tumor burden (FTB). In order to compare across all conditions and dose levels, the FTB is defined as the greatest lower bound of tumor radius over all the single dose experiments, and is approximately $FTB = 5.6\text{mm}$. Because the therapeutic effect of RIT fades over time as the radionuclide decays and the targeted tumor cells are killed, the treatment eventually fails and the tumor returns to a linear radial growth pattern. This can be seen in the single dose experiment by performing linear regression (black lines) on the last 3 time points for each dose level and control. This linear regression is used to calculate the precise time the FTB is attained, indicated with a * on the graph (**Supplemental Figure S9**).

Now we compare the multi-dose ($5.4 \text{ kBq} = 1.85 + 0.70 \times 5 \text{ kBq}$) experiment with the single dose experiments to address the concern that there was not a 5.4 kBq single dose control. So let's look at the growth curve of the multi-dose experiment in comparison to the 3.7 kBq and 7.4 kBq single dose data. We scale the tumor radius of the multi-dose data so that the initial sizes are equal to the 3.7 kBq single dose.

Using the same approach as before, by fitting a line to the last 3 data points in the multi-dose experiment, we extrapolate the growth curve to predict a time of FTB, which falls between the 3.7 kBq and 7.4 kBq single doses. This gives a predicted time to FTB of $T = 71.8$ days. Although the multi-dose tumor radius is consistently larger than the single 3.7 kBq or 7.4 kBq doses, the growth rate overall is significantly reduced.

If we want to predict what would be the result of a 5.4 kBq single dose treatment, we plot the time to FTB versus dose. This plot shows the time to FTB versus Dose for the single dose experiments (**Supplemental Figure S10**).

First, we tried a linear fit to this data, but it didn't look right, and it predicted that more dose would result in longer time to FTB indefinitely, which is clearly not correct. Since we have 4 data points (control (Dose=0) + 3 dose levels) we have enough data to fit a quadratic function. This predicts the time to FTB for a single 5.4 kBq dose, and also

makes an interesting prediction that approximately 9.25 kBq is an optimal dose—in the sense of delaying the time to FTB, not necessarily survival. Beyond that, say 14.8 kBq, we would not predict a benefit in reducing or delaying tumor growth, for example, due to toxicity or very rapid treatment effect resulting in earlier, more rapid tumor re-growth.

The time to FTB for the multi-dose experiment predicted by extrapolating the growth curve is:

T = 71.8 days.

The predicted time to FTB given by the quadratic fit to the single-dose data above is:

T = 71.1 days.

One final question: How do the tumor growth rates compare?

The 5.4 kBq multi-dose has a greatly reduced overall tumor growth rate as compared to the controls and 1.85, 3.7, 7.4 kBq single dose treatments (**Supplemental Figure S11**).

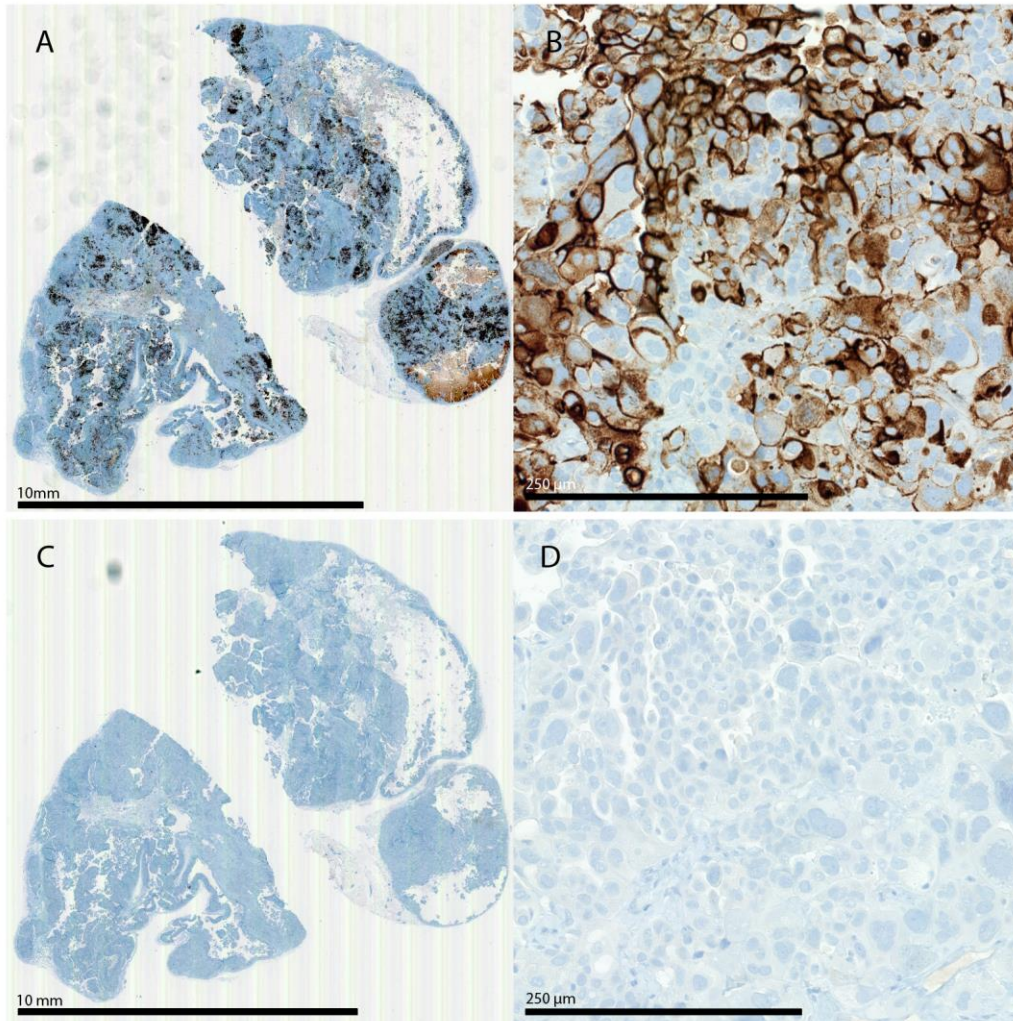
What this means is:

We don't have to do a 5.4 kBq single dose experiment, because

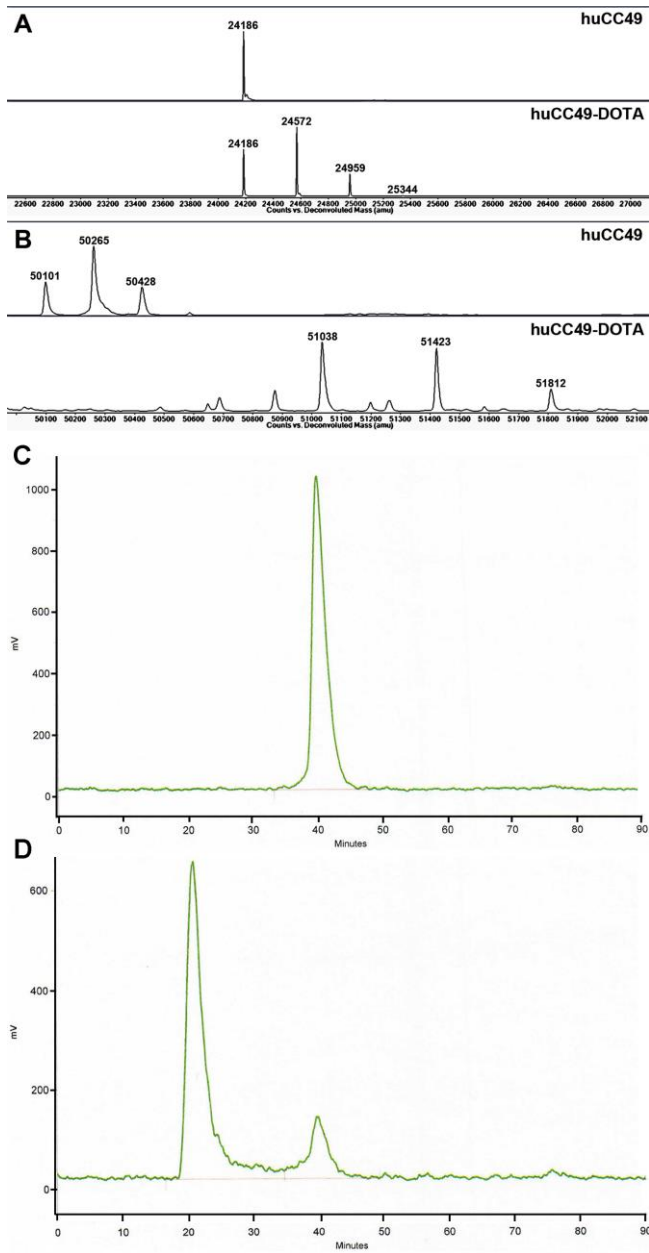
- 1) we can predict what would happen. This is because the overall survival and tumor growth curves are well separated from each other, so we have confidence in interpolating between the dose levels. In other words, 5.4 kBq will be better than 3.7 kBq, but not as good as 7.4 kBq, both in terms of survival and in terms of tumor growth.
- 2) Interestingly, what we predict is that although a single 5.4 kBq dose would have almost exactly the same effect on the time to FTB, our multi-dose experiment has two distinct advantages:
 - a. Less toxicity
 - b. Greatly reduced overall tumor growth rate
 - c. It also has the *potential to mitigate therapeutic resistance

Supplemental Figure 1. TAG-72 expression of OVCAR3 xenografts in NSG mice.

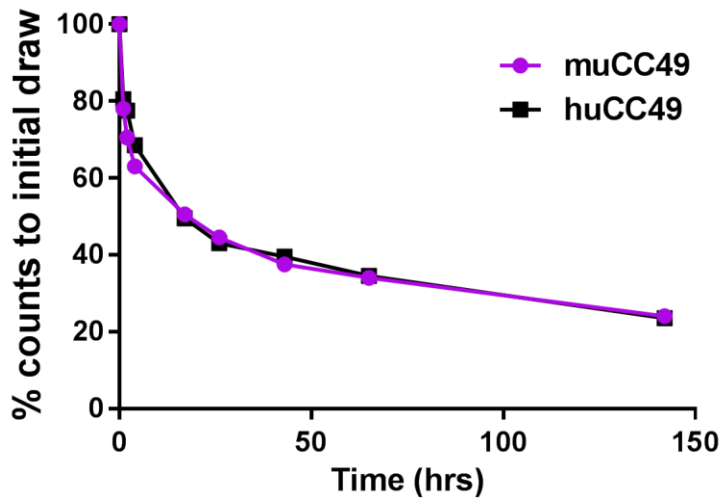
NSG mice with s.c. OVCAR3 xenografts were harvested about 60-90 days post injection and stained with human anti-TAG-72 antibody, huCC49 (A) and (B) or a control anti-CD38 antibody (C) and (D).



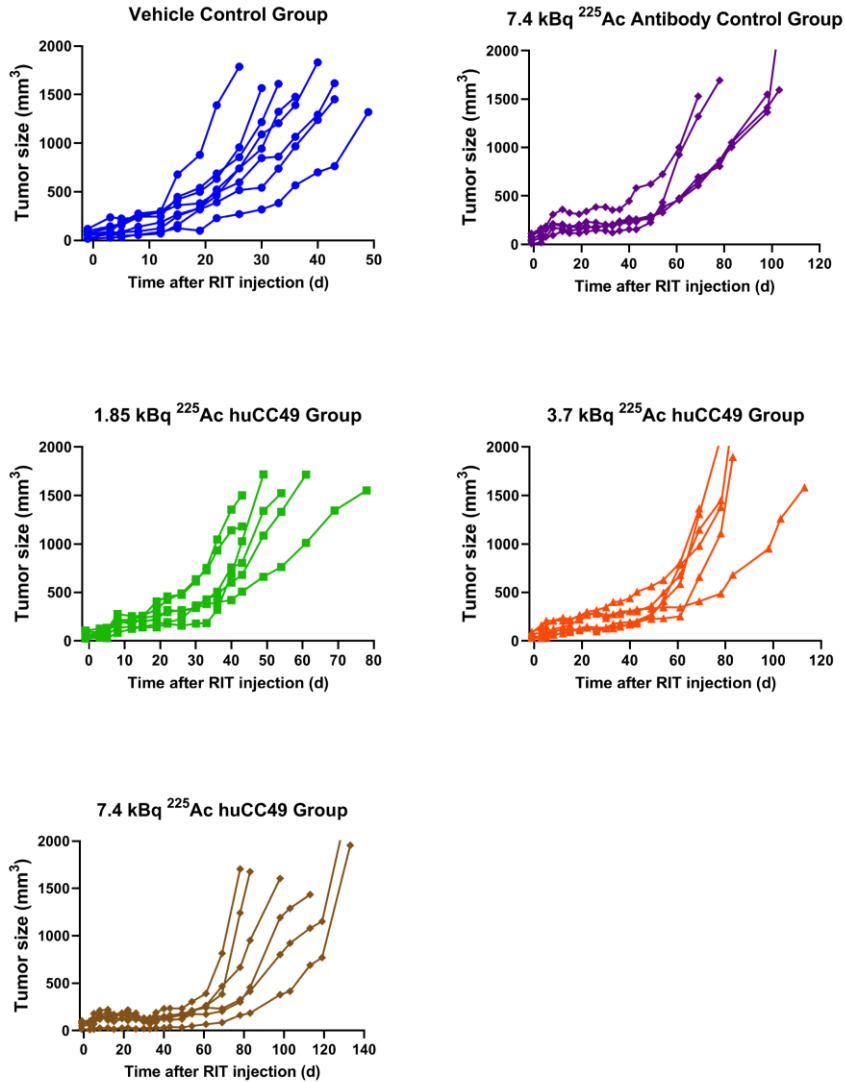
Supplemental Figure 2. Characterization of DOTyated-huCC49. Q-TOF-MS analysis of huCC49 before and after DOTylation. **A.** Light chain before (upper) and after (lower) DOTylation. **B.** Heavy chain before (upper) and after (lower) DOTylation. The average number of DOTA/Ab was calculated as 3.0 from this analysis. Elution of I-124 labeled huCC49 on SEC before (**C**) and after (**D**) addition of 20-fold excess of bovine submaxillary mucin. ITLC of ^{225}Ac -DOTyated-huCC49 showed >95% incorporation with 10 mM DTPA chase (data not shown).



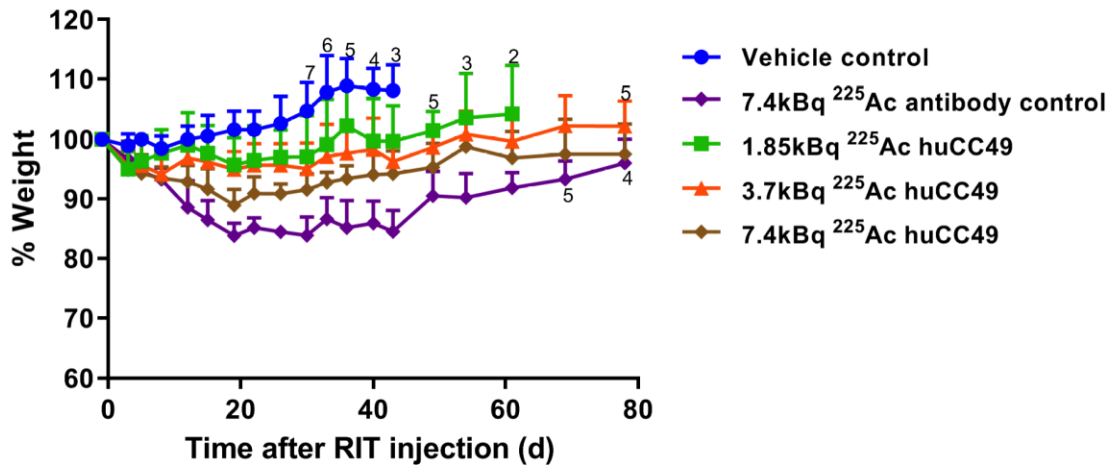
Supplemental Figure 3. Blood Clearance of murine CC49 and humanized CC49. Kinetics of ^{124}I labeled murine or humanized CC49 (370 kBq/mouse) in OVCAR3 xenografted female NSG mice. The average counts in blood are shown in graph (n=2/time point).



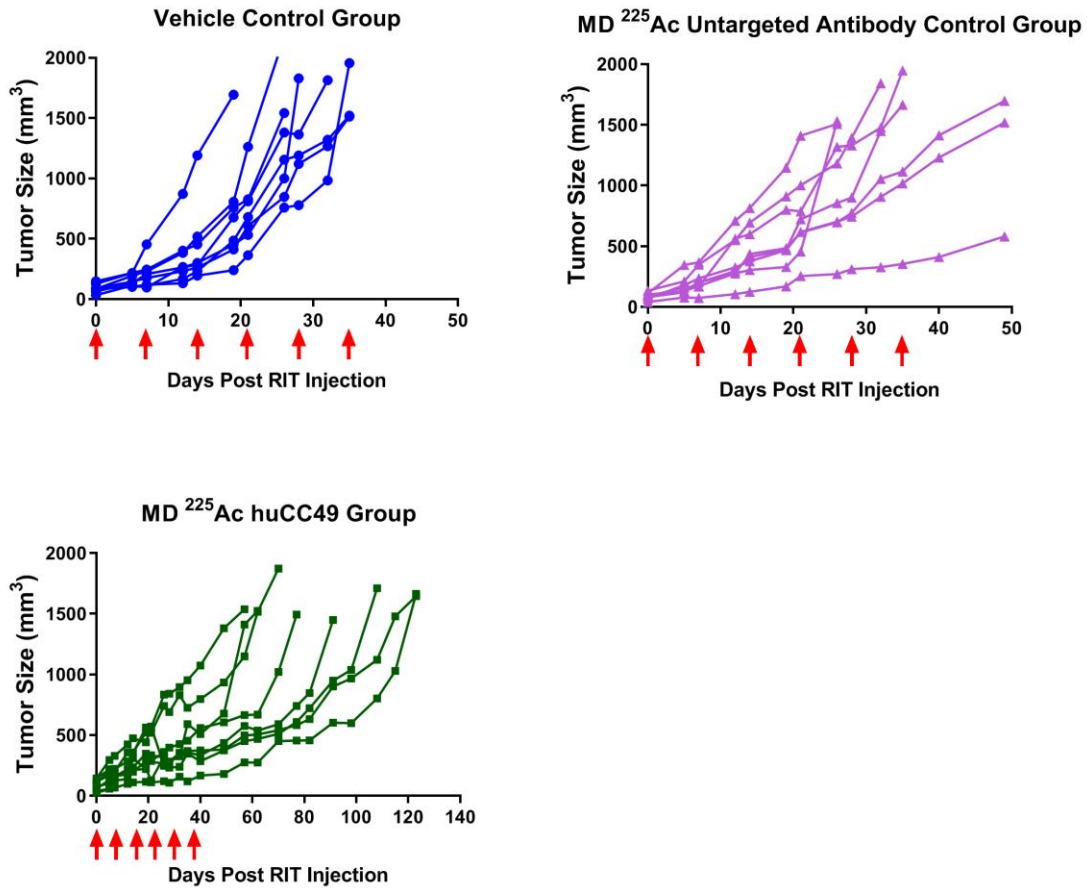
Supplemental Figure 4. Single dose therapy with ^{225}Ac -DOTAylated-huCC49 in OVCAR3 xenografts in female NSG mice. Red arrow indicates day RIT given. Graphs are of individual mice within each treatment group.



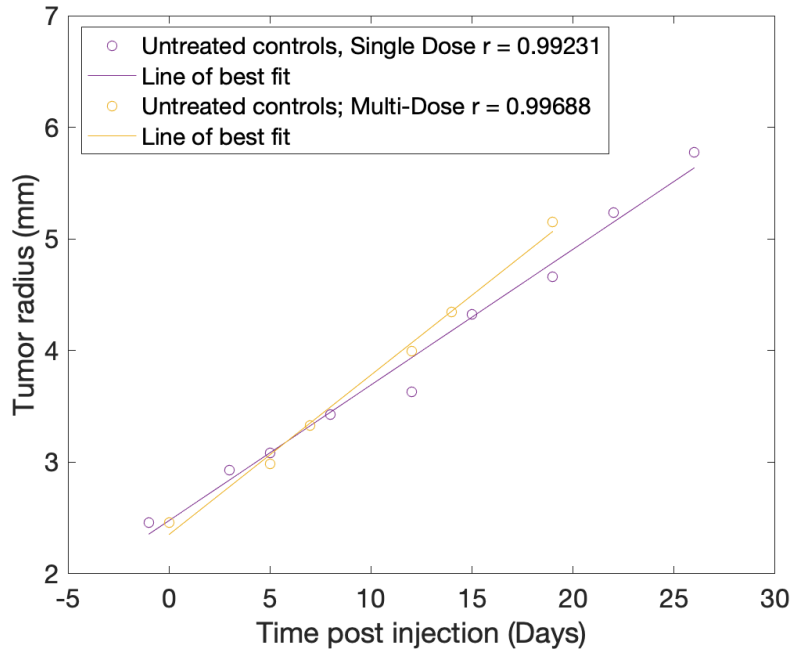
Supplemental Figure 5. Whole body toxicity of single dose RIT in OVCAR3 xenografts in female NSG mice. Toxicity, as measured by weight loss, of the single dose RIT treated groups (n=8 for control group, n=6 for all other groups). The whole body toxicity curves of the 7.4 kBq ²²⁵Ac untargeted antibody control (****, p=<0.0001), 1.85 kBq ²²⁵Ac huCC49 (**, p=0.0067), 3.7 kBq ²²⁵Ac huCC49 (***, p=0.0001), and 7.4 kBq ²²⁵Ac-huCC49 (****, p=<0.0001) groups were statistically significant compared to the vehicle control. Statistics were carried out using one-way ANOVA, up to day 43.



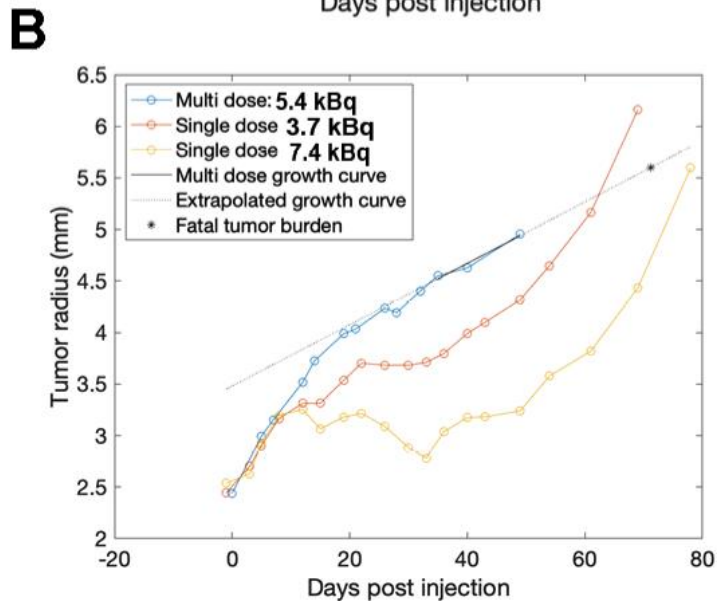
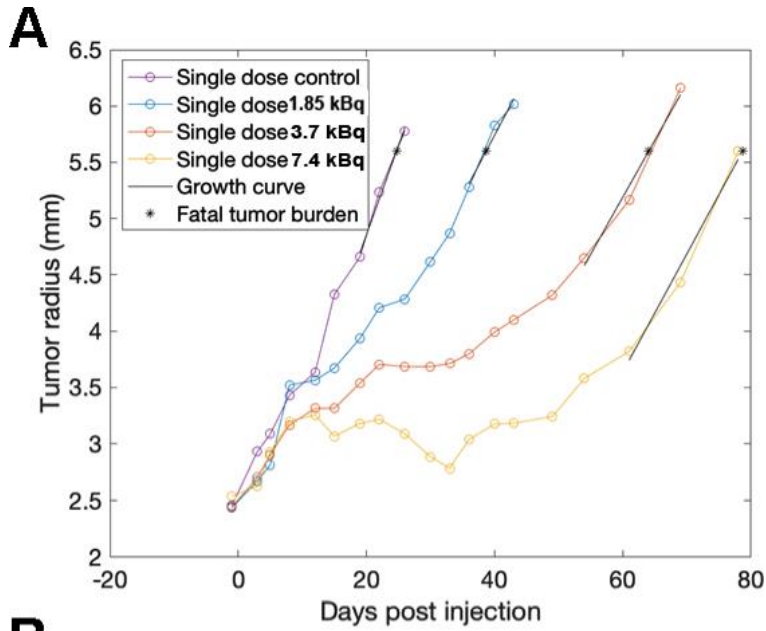
Supplemental Figure 6. Multi-dose therapy ^{225}Ac -DOTAylated-huCC49 in OVCAR3 xenografts in female NSG mice. Doses were given at day 0, day 7, day 14, day 21, day 28, and day 35. Graphs are of individual mice within each treatment group (n=8 for all groups).



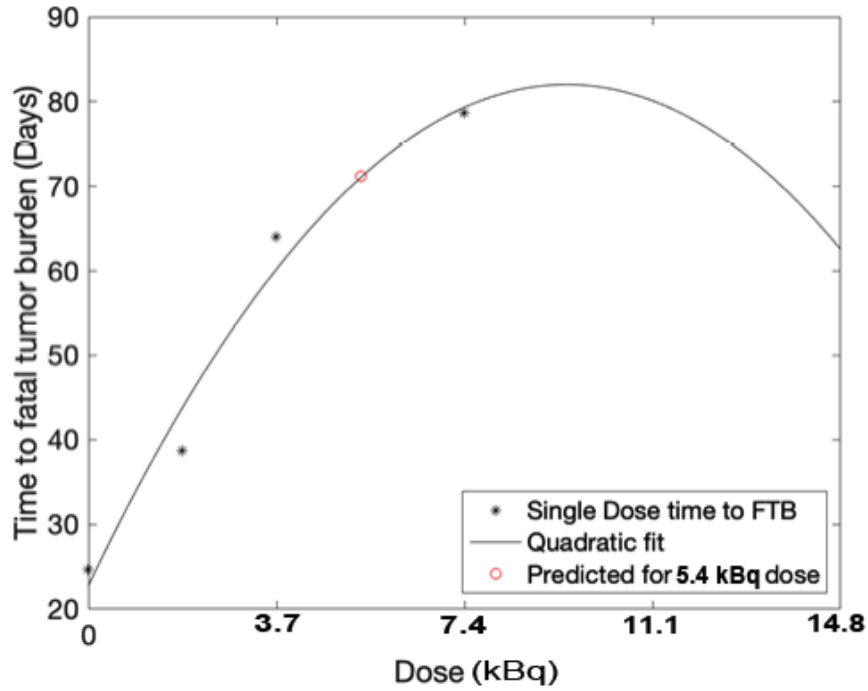
Supplemental Figure 8. Calculated average tumor volume across all mice for each time point and treatment condition. There is a linear correlation of tumor radius with time of treatment.



Supplemental Figure 9. A linear regression analysis to calculate the precise time the FTB is attained. A. Time to fatal tumor burden (FTB) for single doses. **B.** Time to FTB with multiple dose included.



Supplemental Figure 10. Plot of time to FTB versus dose. Data was fitted to a quadratic equation.



Supplemental Figure 11. Graph of tumor growth rate vs dose. All of the tumor growth rates except for the 5.4 kBq dose are shown for single treatments. The 5.4 kBq growth rate was for the multi-treatment strategy.

